Acta Oceanol. Sin., 2022, Vol. 41, No. 10, P. 22–31
https://doi.org/10.1007/s13131-022-2000-x
http://www.aosocean.com
E-mail: ocean2@hyxb.org.cn

FIO-ESM v2.0 CORE2-forced experiment for the CMIP6 Ocean Model Intercomparison Project

Qi Shu[1, 2, 3], Zhenya Song[1, 2, 3], Ying Bao[1, 2, 3], Xiaodan Yang[1, 2, 3], Yajuan Song[1, 2, 3], Xinfang Li[1], Meng Wei[1, 2, 3], Fangli Qiao[1, 2, 3]*

[1] First Institute of Oceanography, and Key Laboratory of Marine Science and Numerical Modeling, Ministry of Natural Resources, Qingdao 266061, China

[2] Laboratory for Regional Oceanography and Numerical Modeling, Pilot National Laboratory for Marine Science and Technology (Qingdao), Qingdao 266237, China

[3] Shandong Key Laboratory of Marine Science and Numerical Modeling, Qingdao 266061, China

Received 16 September 2021; accepted 29 November 2021

© Chinese Society for Oceanography and Springer-Verlag GmbH Germany, part of Springer Nature 2022

Abstract

We introduced the Coupled Model Intercomparison Project Phase 6 (CMIP6) Ocean Model Intercomparison Project CORE2-forced (OMIP-1) experiment by using the First Institute of Oceanography Earth System Model version 2.0 (FIO-ESM v2.0), and comprehensively evaluated the simulation results. Unlike other OMIP models, FIO-ESM v2.0 includes a coupled ocean surface wave component model that takes into account non-breaking surface wave-induced vertical mixing in the ocean and effect of surface wave Stokes drift on air-sea momentum and heat fluxes in the climate system. A sub-layer sea surface temperature (SST) diurnal cycle parameterization was also employed to take into account effect of SST diurnal cycle on air-sea heat fluxes to improve simulations of air-sea interactions. Evaluations show that mean values and long-term trends of significant wave height were adequately reproduced in the FIO-ESM v2.0 OMIP-1 simulations, and there is a reasonable fit between the SST diurnal cycle obtained from *in situ* observations and that parameterized by FIO-ESM v2.0. Evaluations of model drift, temperature, salinity, mixed layer depth, and the Atlantic Meridional Overturning Circulation show that the model performs well in the FIO-ESM v2.0 OMIP-1 simulation. However, the summer sea ice extent of the Arctic and Antarctic is underestimated.

Key words: FIO-ESM, OMIP, CMIP6, OGCM

Citation: Shu Qi, Song Zhenya, Bao Ying, Yang Xiaodan, Song Yajuan, Li Xinfang, Wei Meng, Qiao Fangli. 2022. FIO-ESM v2.0 CORE2-forced experiment for the CMIP6 Ocean Model Intercomparison Project. Acta Oceanologica Sinica, 41(10): 22–31, doi: 10.1007/s13131-022-2000-x

1 Introduction

The Ocean Model Intercomparison Project (OMIP) is an endorsed project in the Coupled Model Intercomparison Project Phase 6 (CMIP6) (Eyring et al., 2016). It addresses CMIP6 science questions, investigating origins and consequences of systematic model biases (Griffies et al., 2016). It also provides an important framework for evaluating (including assessment of systematic biases), understanding, and improving ocean, sea-ice, tracer, and biogeochemical components of climate and earth system models contributing to CMIP6 (Griffies et al., 2016). The OMIP experiments have two components: the physical component and the biogeochemical component. We only focus on the physical component in this study. It follows the Coordinated Ocean-ice Reference Experiments (CORE-I and CORE-II) (Griffies et al., 2009; Danabasoglu et al., 2014), which are the standard methods to evaluate global ocean/sea ice simulations and to examine mechanisms for forced ocean climate variability. More than 60 models have registered for the CMIP6 OMIP.

The First Institute of Oceanography Earth System Model version 2.0 (FIO-ESM v2.0) is one of the contributors to the OMIP. The main difference between FIO-ESM v2.0 and other OMIP models is that FIO-ESM v2.0 couples an ocean surface wave model. The FIO-ESM v2.0 (Bao et al., 2020) is the successor to FIO-ESM v1.0 (Qiao et al., 2013); both versions have been developed by the First Institute of Oceanography, Ministry of Natural Resources, China, and coupled ocean surface wave component model. Its fully coupled CMIP6 historical simulations demonstrate good model performance in terms of simulations of surface air temperature, precipitation, sea surface temperature (SST), Atlantic Meridional Overturning Circulation (AMOC), and El Niño-Southern Oscillation (Bao et al., 2020).

The aim of this study is to introduce the FIO-ESM v2.0 CORE2-forced (OMIP-1) experiment, and evaluate its performance. The paper is structured as follows. The model and numerical experiment are described in Section 2, results are presented and evaluated in Section 3, summary and discussion are provided in Section 4.

Foundation item: The National Key R&D Program of China under contract Nos 2018YFA0605701 and 2016YFB0201100; the National Natural Science Foundation of China under contract Nos 41941012 and 41821004; the Basic Scientific Fund for National Public Research Institute of China (ShuXingbei Young Talent Program) under contract No. 2019S06.
*Corresponding author, E-mail: qiaofl@fio.org.cn

2 Model and experiment description

2.1 *Model*

The FIO-ESM v2.0 is a fully coupled earth system model (Bao et al., 2020). Its three component models, i.e., the ocean general circulation model (OGCM), sea ice model, and ocean surface wave model, are employed in the OMIP simulation. The OGCM used in FIO-ESM is the Parallel Ocean Program (POP2) (Smith et al., 2010). It has 61 vertical layers (z) in FIO-ESM v2.0, with the first layer at 0 m with SST diagnosed by the SST diurnal cycle parameterization (Yang et al., 2017). Horizontal resolution is approximately 1.1° in longitude and 0.27°–0.54° in latitude. The sea ice model is the Los Alamos sea ice model version 4 (CICE4) (Bailey et al., 2011). It has one snow layer, four vertical ice layers, and five ice thickness categories in FIO-ESM v2.0. The ocean surface wave model is the Marine Science and Numerical Modeling (MASNUM) surface wave model (Qiao et al., 2016). It has 12 wave directions and 25 wave numbers in FIO-ESM v2.0. All three component models have the same horizontal resolution. The coupler used in FIO-ESM v2.0 is CPL7 (Craig et al., 2012). POP2 and MASNUM wave model exchange data with the coupler every 3 h, and CICE4 exchanges data with the coupler every 30 min.

Ocean surface waves can be simulated directly in FIO-ESM v2.0 by the coupled MASNUM wave model, allowing FIO-ESM v2.0 to take into account the wave related processes on the climate system. Non-breaking surface wave-induced mixing and effect of surface wave Stokes drift on air-sea momentum and heat fluxes are two important ocean surface wave related processes that are taken into account in the FIO-ESM v2.0 OMIP-1 simulation, and represent the main differences between FIO-ESM v2.0 and all other OMIP models.

Previous studies show that non-breaking surface wave-induced mixing is a key process to improve upper ocean temperature and mixed layer depth (MLD) simulations both in summer (Qiao et al., 2010; Wang et al., 2010, 2019; Shu et al., 2011) and in winter (Chen et al., 2018). Overestimates of summer SST and underestimates of summer mixed layer depth in OGCMs can be addressed by including the non-breaking surface wave-induced vertical mixing. Following Qiao et al. (2004), non-breaking surface wave-induced mixing is calculated in FIO-ESM v2.0 using wave-number spectrum from the MASNUM wave model, and then added to the vertical viscosity and diffusivity coefficients parameterized by the K-Profile Parameterization (KPP) vertical mixing scheme (Large et al., 1994) in POP2.

In the bulk formula, the turbulent fluxes (wind stress, evaporation, latent heat flux, and sensible heat flux) are parameterized using the difference between near surface wind velocity and ocean surface current (Large and Yeager, 2009). In the real ocean, surface current also includes Stokes drift velocity, which is induced by ocean surface waves. Although velocity decays rapidly with depth, surface velocity is comparable with surface Ekman current (Rascle et al., 2008). Effects of surface wave Stokes drift on air-sea momentum and heat fluxes are considered in FIO-ESM v2.0 by adding surface Stokes drift velocity to the first layer ocean current during turbulent flux parameterization (Bao et al., 2020). Using wave-number spectrum in the MASNUM wave model, Stokes drift velocity is calculated following the formula of Huang (1971).

Effect of wave-induced sea spray on air-sea heat and water fluxes is another important ocean surface wave related process included in FIO-ESM v2.0 (Bao et al., 2020). However, it is deactivated during the OMIP simulation, because it is absent from the bulk formulae (Large and Yeager, 2009) for air-sea turbulent heat flux calculation prescribed for CMIP6 OMIP experiments.

Previous studies suggest that the SST diurnal cycle can affect the climatology, intra-seasonal, and inter-annual variability of the climate system by modulating air-sea interactions (Danabasoglu et al., 2006; Bernie et al., 2008; Ham et al., 2010; Masson et al., 2012). However, vertical resolution in the upper ocean of most climate models and OGCMs is too low to resolve the SST diurnal cycle. In FIO-ESM v2.0, diurnal signals of SST at 0 m are diagnosed using a sub-layer parameterization of the SST diurnal cycle (Yang et al., 2017; Bao et al., 2020), and are used to calculate air-sea heat fluxes to simulate the effect of the SST diurnal cycle and improve simulations of air-sea interactions.

In the FIO-ESM v2.0 OMIP-1 experiment, three processes including the non-breaking surface wave-induced mixing in the upper ocean, the effects of surface wave Stokes drift on the air-sea momentum and heat fluxes, and the effects of the SST diurnal cycle on air-sea interactions are introduced for the first time in the world, which are the main differences between FIO-ESM v2.0 OMIP-1 experiment and all other OMIP-1 experiments using ocean component model of POP.

2.2 *The experiment*

The OMIP has two versions in the framework of CMIP6, and they are CORE2-forced version (OMIP-1) and JRA55-do-forced version (OMIP-2), respectively. The CORE2 forcing contains the inter-annually varying atmospheric forcing and river runoff of Large and Yeager (2009), which have been developed from NCEP/NCAR (National Centers for Environmental Prediction/National Center for Atmospheric Research) reanalysis, Dai and Trenberth (2002) and Dai et al. (2009). This forcing covers 1948 to 2009, but has not been updated since 2009. The JRA55-do forcing (Tsujino et al., 2018) is based on the Japanese Reanalysis (JRA-55) product from Kobayashi et al. (2015). This forcing covers 1958 to 2018, and is updated regularly.

FIO-ESM v2.0 CORE2-forced experiment is a standard OMIP-1 experiment. CORE2 forcing includes surface wind, surface air temperature and specific humidity at 10 m height, sea level pressure, downward shortwave radiation, downward longwave radiation, and precipitation (rain and snow), mostly at 6-hourly intervals. Surface turbulent fluxes were calculated from oceanic state, prescribed atmospheric state, and bulk formulae of Large and Yeager (2009). SST was not restored, and sea surface salinity was restored to monthly observational-based climatology with a piston velocity of 50 m over 4 years. Initial temperature and salinity for the ocean model were taken from the climatology of World Ocean Atlas 2013 version 2 (WOA13v2) (Locarnini et al., 2013; Zweng et al., 2013). For the upper 1 500 m, January climatology was used. Below a depth of 1 500 m, the average of January, February, and March was used. Initial ocean velocity and ocean surface wave started from a state of rest. The simulation was run for five cycles over the period covered by CORE2 forcing (1948–2009 with 62 years for each cycle) to remove dependence on initial conditions and to reach quasi-equilibrium in the upper ocean.

3 Results

In this section, results from FIO-ESM v2.0 OMIP-1 simulations are evaluated. We use results from all five cycles to evaluate model drift, and results from the last cycle to assess model bias and performance.

3.1 *Long-term drift*

Griffies et al. (2009) and Tsujino et al. (2020) showed that long-term drifts always exist in OGCMs after initialization. Long-

term temperature and salinity drifts in the FIO-ESM v2.0 OMIP-1 simulation are shown in Fig. 1. Drifts in global mean vertically averaged potential temperature and salinity in the FIO-ESM v2.0 OMIP-1 simulation are small with mean rates of –0.02°C/(100 a) and –0.000 1/(100 a), respectively. However, similar to other OMIP models (Tsujino et al., 2020), drifts are relatively large both in the upper ocean, and from the deep ocean of 4 000 m to the ocean bottom (Fig. 1a). After initialization, simulated temperature increases in the upper ocean, and decreases in the deep ocean down to the ocean bottom. Salinity drifts mainly in the subsurface ocean between depths of 400 and 1 000 m. Figure 1 also shows that model drift is quite small for the upper 2 000 m in the last (fifth) cycle, indicating quasi-equilibrium in the upper ocean.

The AMOC index and Global Meridional Overturning Circulation (GMOC) index can be used as circulation metrics to quantify model drift (Tsujino et al., 2020). The AMOC index is defined as the vertical maximum of the Atlantic streamfunction at 26.5°N, and represents the strength of the AMOC associated with the formation of North Atlantic Deep Water (NADW). The GMOC index is defined as the minimum of the global streamfunction between 2 000 m depth and the ocean bottom at 30°S, and represents the strength of deep GMOC associated with the formation of Antarctic Bottom Water (AABW) and Lower Circumpolar Deep Water. Figure 2 shows that AMOC decreases in the first cycle after initialization, and recovers gradually thereafter. Model spin-up takes about three cycles. So we suggest that the fourth and fifth cycles of FIO-ESM v2.0 OMIP-1 results are suitable for further scientific analysis. For the last cycle, mean value for the AMOC index is 16.5×10^6 m^3/s and mean value for the GMOC index is -9.9×10^6 m^3/s, and are similar to the multi-model mean values from 11 OMIP-1 models reported by Tsujino et al. (2020).

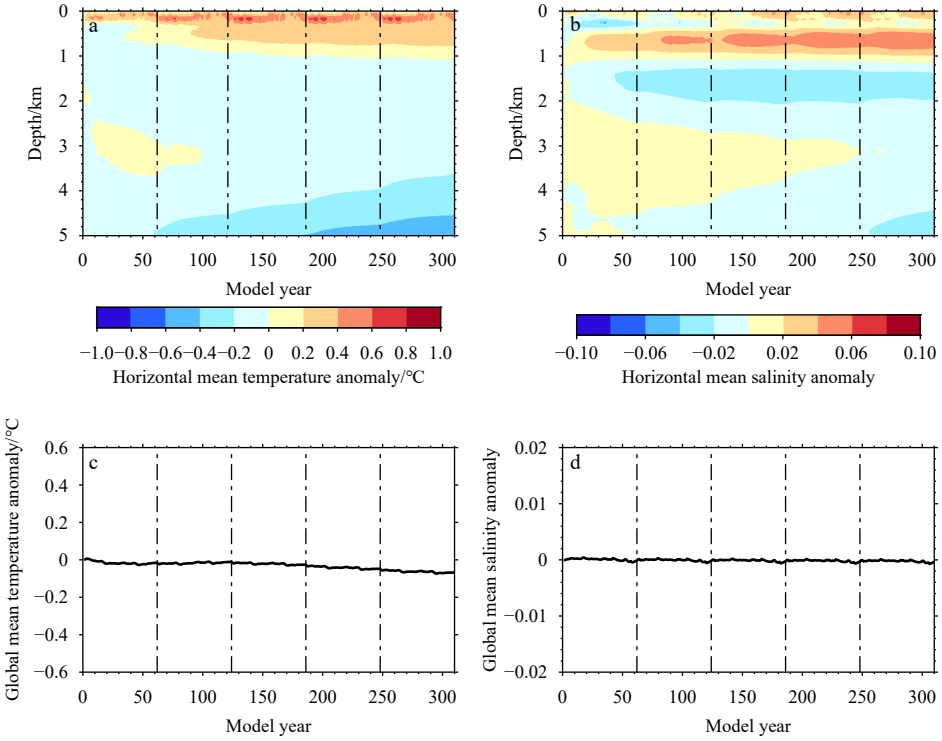

Fig. 1. Drifts of horizontal and global mean potential temperature and salinity. Drift is defined as deviation from the value obtained from the first model year. Dashed lines indicate the 62-year forcing cycle, corresponding to calendar years 1948–2009, which was repeated for 5 times.

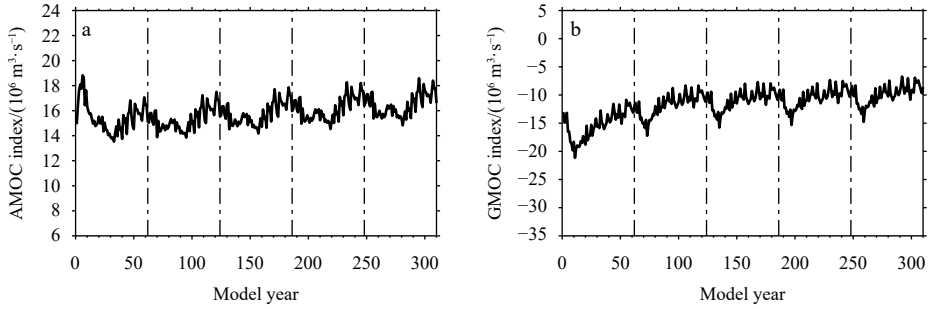

Fig. 2. Time series of annual mean Atlantic Meridional Overturning Circulation (AMOC) index maximum at 26.5°N (a) and Global Meridional Overturning Circulation (GMOC) index minimum between 2 000 m depth and ocean bottom at 30°S (b). Dashed lines indicate the 62-year forcing cycle, corresponding to calendar years 1948–2009, which was repeated.

3.2 *Evaluation of OGCM*

Model biases of zonally averaged temperature, salinity, and biases of SST and sea surface salinity (SSS) in Figs 3 and 4 show that simulation errors of temperature and salinity are small in most oceans except for the Arctic Ocean. For potential temperature, model biases are below 0.5°C in most regions, and are relatively high (>0.5°C) in the intermediate layer of (400–2 000 m) the Arctic Ocean and subsurface (100–400 m) tropical oceans. The large temperature biases in the intermediate layer of the Arctic Ocean also appear in CORE-II and CMIP5 models (Ilıcak et al., 2016; Shu et al., 2019), possibly because of large temperature anomalies in the Atlantic Water entering the Arctic Ocean through the Fram Strait (Ilıcak et al., 2016). For salinity, model biases are less than 0.1 psu in most oceans, but simulated salinity in the Arctic Ocean subsurface (50–400 m) is lower than the observed climatology from WOA13v2 (Fig. 3b). The negative salinity biases in the subsurface Arctic Ocean can also be found in almost all the CORE-II models (Fig. 7 in Ilıcak et al., 2016), possibly because of problems in the parameterization of brine formation and descent of high-salinity water masses into the interior of the Arctic Ocean (Ilıcak et al., 2016).

Mixed layer depth in the upper ocean is one of the most important ocean variables in the global climate system. It can directly affect air-sea fluxes of heat, freshwater, greenhouse gases, and can be defined as the depth where ocean potential density deviates from its value at the surface by 0.03 kg/m^3. We used the gridded monthly climatological MLD dataset from the observations of de Boyer Montégut et al. (2004) to evaluate the performance of the FIO-ESM v2.0 OMIP-1 simulation. Since MLD has a marked seasonal cycle, we selected January, February, and March as the typical months of boreal winter (austral summer), and July, August, and September as the typical months of boreal summer (austral winter).

Including the non-breaking surface wave-induced mixing in the vertical mixing scheme of POP can reduce simulated sea surface temperature and increase subsurface temperature of the upper ocean in summer, which can deepen MLD and improve mixed layer simulations (Huang et al., 2012). Figure 5 suggests that the FIO-ESM v2.0 OMIP-1 simulation can reasonably reproduce the spatial patterns and seasonal cycles of observed MLD. There is a good fit between observations and the simulation in the oceans at low and middle latitudes. However, MLD in the Southern Ocean in the FIO-ESM v2.0 OMIP-1 simulation is still shallower than that from observations, which is a discrepancy that has also been noted in CORE-II and CMIP5 models (Huang et al., 2014; Downes et al., 2015). In winter, increase of MLD depth in the Northern Atlantic and Southern Ocean is reproduced in the FIO-ESM v2.0 OMIP-1 simulation. However, simulated MLD in the Northern Atlantic is larger and simulated MLD in the Southern Ocean is smaller relative to observations.

The AMOC simulations from the FIO-ESM v2.0 OMIP-1 experiment are shown in Fig. 6. The AMOC consists of two primary

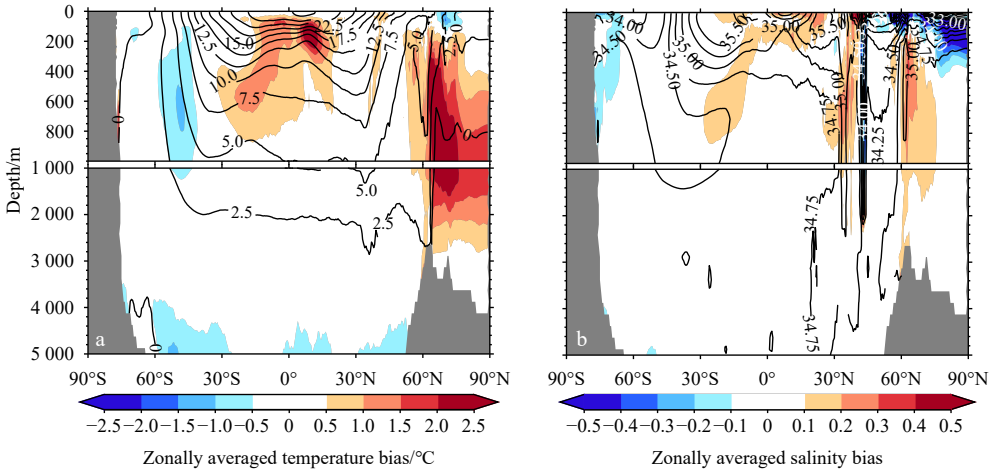

Fig. 3. Biases of zonally averaged temperature (a) and salinity (b) from the last cycle of the FIO-ESM v2.0 OMIP-1 simulation relative to observed climatological values from World Ocean Atlas 2013 version 2 (WOA13 v2). Black contour is zonally averaged temperature and salinity from WOA13v2.

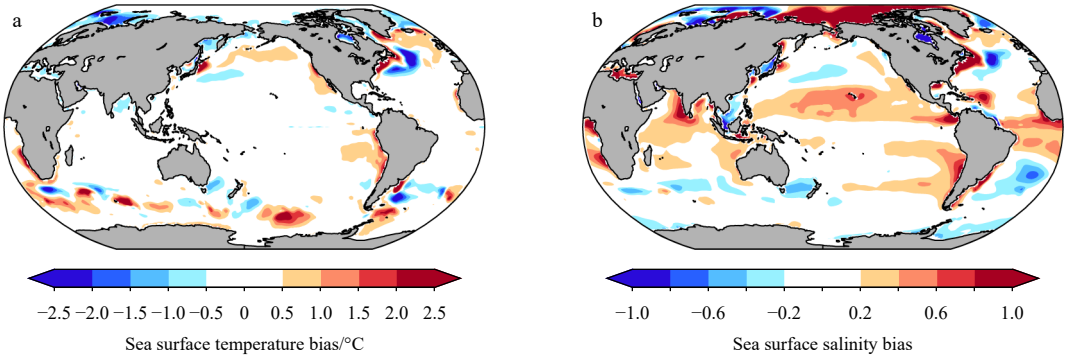

Fig. 4. Biases of sea surface temperature (a) and salinity (b) from the last cycle of the FIO-ESM v2.0 OMIP-1 simulation relative to observed climatological values from World Ocean Atlas 2013 version 2 (WOA13 v2).

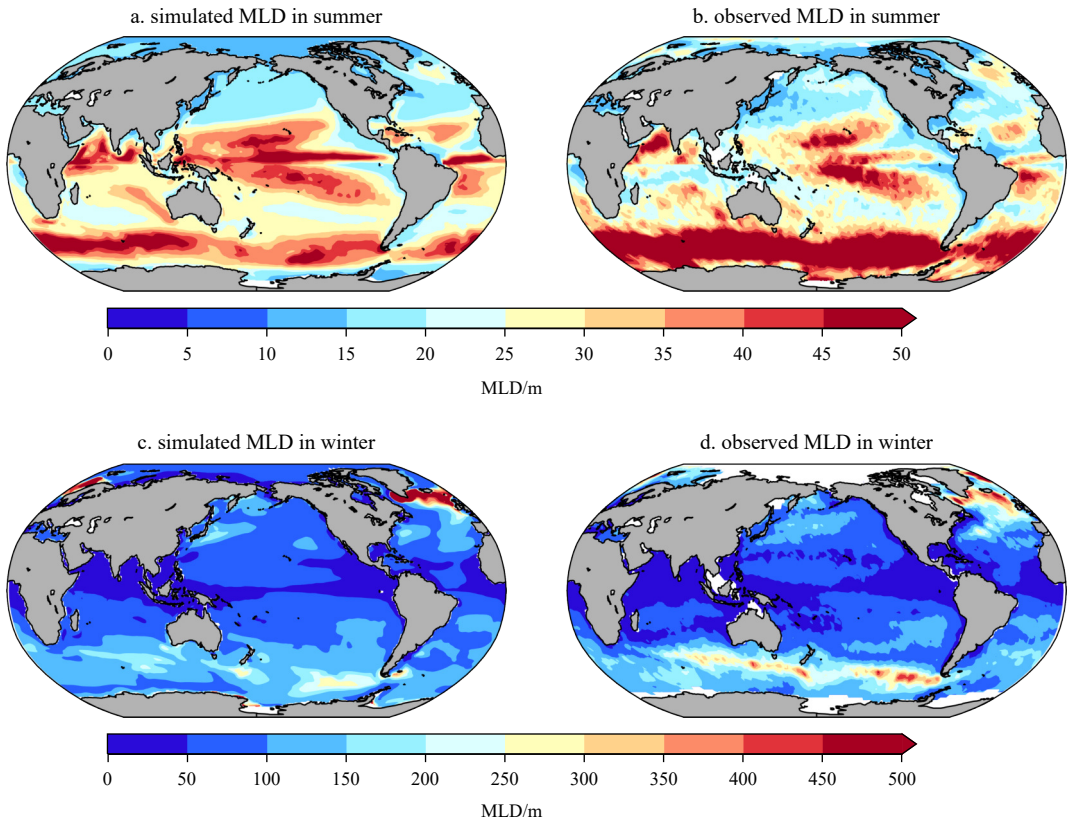

Fig. 5. Simulated and observed mixed layer depth (MLD) in summer and winter. Mixed layer depth is defined as the depth where ocean potential density deviates from its value at the surface by 0.03 kg/m^3. The average of January, February, and March is selected as the typical months for boreal winter (austral summer), and the average of July, August, and September is selected as the typical months for boreal summer (austral winter). Observations are from de Boyer Montégut et al. (2004).

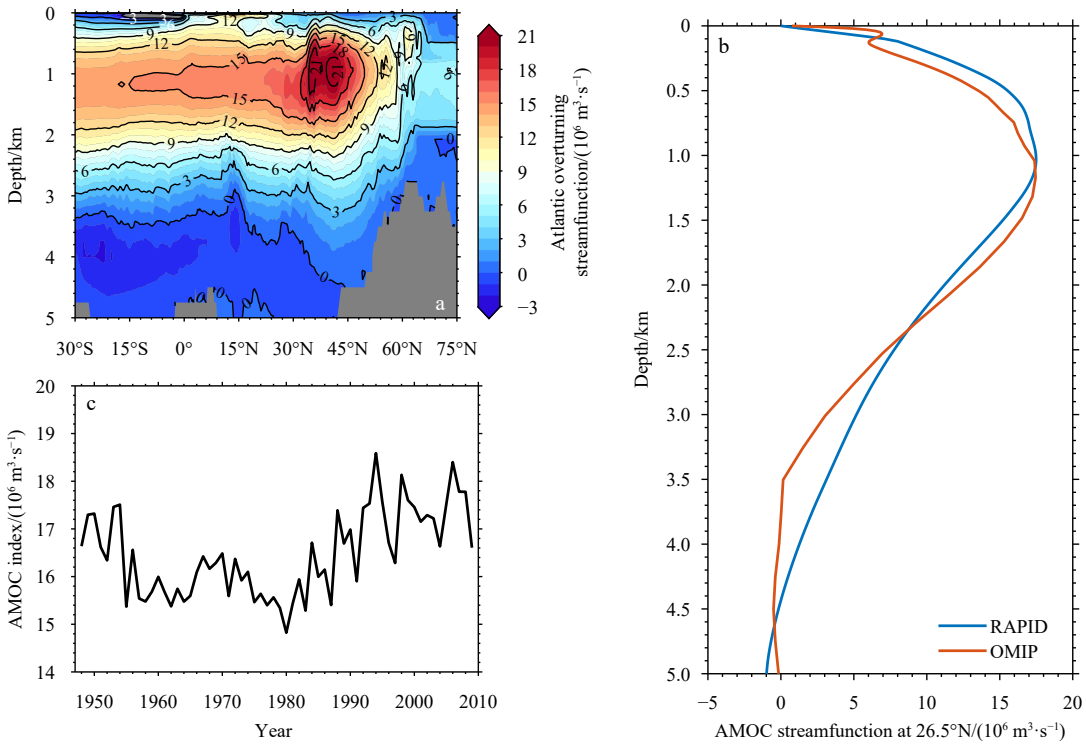

Fig. 6. Atlantic overturning streamfunction from the last cycle of the FIO-ESM v2.0 OMIP-1 simulation (a), AMOC streamfunction profiles (brown line: FIO-ESM v2.0 OMIP-1 simulation, blue line: RAPID observations) at 26.5°N between 2004 and 2009 (b), and AMOC index from the last cycle of the FIO-ESM v2.0 OMIP-1 simulation (c).

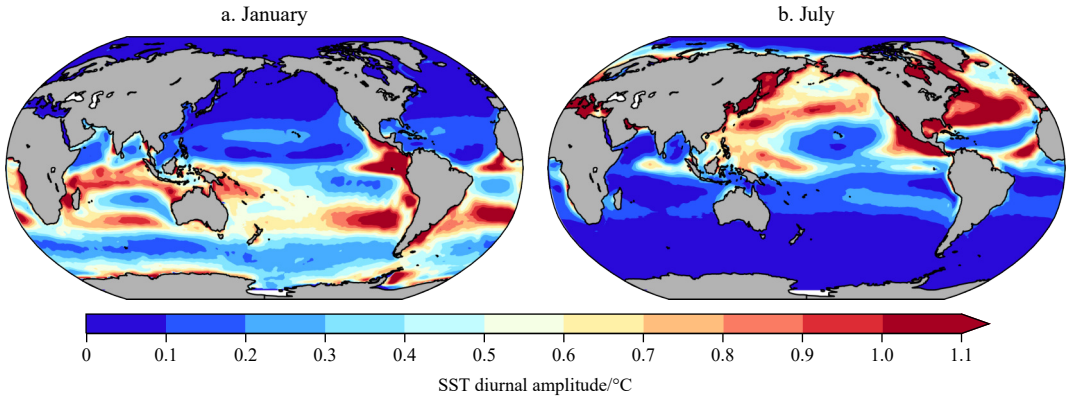

Fig. 7. Diurnal amplitude of sea surface temperature (SST) in January (a) and July (b) in the last cycle of the FIO-ESM v2.0 OMIP-1 simulation. Diurnal amplitude of SST is defined as the difference between maximum and minimum of SST in the same day.

overturning cells (Lumpkin and Speer, 2007). The upper cell transports warm water northward in the upper layers to compensate for NADW formation and returns southward. In the deep cell, AABW flows northward and rises into the lower part of the southward-flowing NADW. Figure 6a shows that these two cells are adequately reproduced in the FIO-ESM v2.0 OMIP-1 simulation. Figure 6b shows a good fit between the AMOC streamfunction profile at 26.5°N from the FIO-ESM v2.0 OMIP-1 simulation and that from Rapid Climate Change (RAPID) observations (Frajka-Williams et al., 2021). The fit between simulation and observations is superior to that obtained from most CORE-II models (Fig. 5 in Danabasoglu et al., 2014). The time series of the AMOC index shown in Fig. 6c indicates that AMOC strength varies interannually and decadally, which is consistent with results from other CORE-II and OMIP-1 simulations (Danabasoglu et al., 2016; Tsujino et al., 2020), although validation with observations is impossible because of lack of long-term observations.

The SST diurnal cycle can be reproduced in FIO-ESM v2.0 because of a sub-grid parameterization of the cycle. We used SST diurnal amplitude to assess model simulation of the SST diurnal cycle. Diurnal amplitude of SST is defined as the difference between maximum and minimum SST in the same day. Figure 7 indicates the presence of a marked seasonal cycle with SST diurnal amplitude being larger in summer (January) and smaller in winter (July). In many regions, amplitudes are large and exceed 1°C. Amplitudes are large in tropical and mid-latitude oceans in the southern Hemisphere in January, and in the northern Hemisphere in July. Because of strong wind and low shortwave radiation, amplitudes are quite small in winter. The characteristics of the spatial distribution and seasonal variation of the SST diurnal amplitude shown in Fig. 7 are basically consistent with the results of previous studies (Kawai and Wada, 2007; Clayson and Weitlich, 2007).

To evaluate model bias in mean SST diurnal amplitude, we compared model output with observations made between 2002 and 2009 by 107 moorings as part of the Tropical Ocean Global Atmosphere/Coupled Ocean Atmosphere Response Experiment (TOGA/COARE, Webster and Lukas, 1992) (Fig. 8). Mean model error in SST diurnal amplitude is 0.08°C, and relative mean error is 19%. Correlation coefficient (Spearman's rho) between model output and observations is 0.91.

3.3 *Evaluation of sea ice model*

Sea ice extent is one of the most important variables used to evaluate sea ice model performance. It can be calculated as the

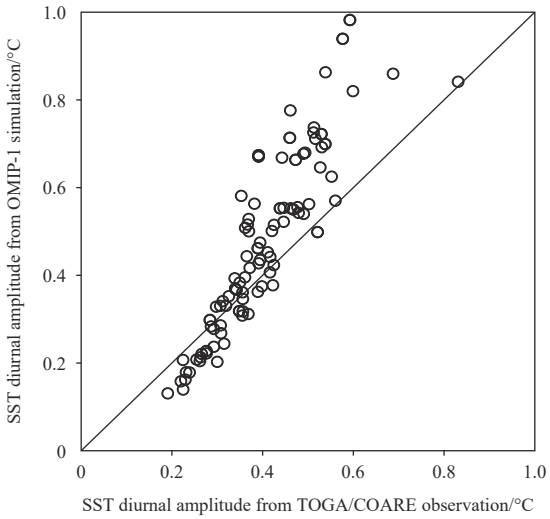

Fig. 8. Scatter plot of mean sea surface temperature (SST) diurnal amplitude between 2002 and 2009 from the FIO-ESM v2.0 OMIP-1 simulation and from observations of 107 moorings as part of TOGA/COARE.

sum of the area where sea ice concentration exceeds 15%. Observations show that Arctic sea ice extent is largest in March and smallest in September, while Antarctic sea ice extent is largest in September and smallest in February. We compared satellite-derived sea ice extent with simulated Arctic sea ice extent in March and September, and Antarctic sea ice extent in February and September. The satellite-derived sea ice extent is from National Snow and Ice Data Center (Fetterer et al., 2017). Figure 9 shows winter sea ice extent from the FIO-ESM v2.0 OMIP-1 simulation fits the satellite observations. However, the model underestimates sea ice extent in both hemispheres in summer. Tsujino et al. (2020) suggests that the negative biases of summer sea ice concentration can be considerably reduced by using the JRA55-do atmospheric forcing in both hemispheres. Although simulated mean sea ice extent is smaller than observed mean sea ice extent, the rapid decline of summer Arctic sea ice extent observed during the satellite era is reproduced in the simulation. Linear trends of September sea ice extent between 1979 and 2009 from satellite observations and the FIO-ESM v2.0 OMIP-1 simulation are -0.74×10^6 km^2/decade and -0.90×10^6 km^2/decade, respectively.

The model underestimates Arctic summer sea ice extent,

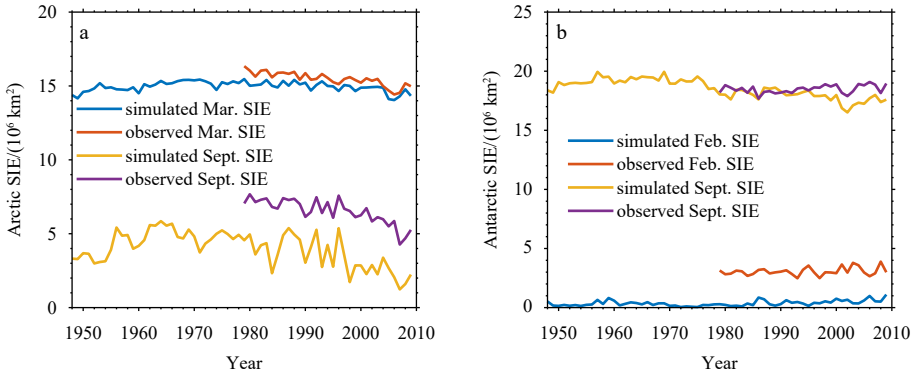

Fig. 9. Arctic (a) and Antarctic (b) sea ice extent (SIE) from the last cycle of the FIO-ESM v2.0 OMIP-1 simulations and satellite-derived observations. Sea ice extent is calculated as the sum of the area where sea ice concentration exceeds 15%.

which can be a result of underestimation of winter ice thickness despite an adequate reproduction of sea ice extent. Simulated ice thickness from the FIO-ESM v2.0 OMIP-1 simulation is lower than that from the Pan-Arctic Ice-Ocean Modeling and Assimilation System (PIOMAS) dataset (Zhang and Rothrock, 2003) (Fig. 10). Sea ice thickness in the Arctic Basin over 1978 and 2009 exceeds 2 m in March from PIOMAS, and is below 2 m for most regions in the FIO-ESM v2.0 OMIP-1 simulation. Therefore, the sea ice model in FIO-ESM v2.0 needs further improvement in the future.

3.4 *Evaluation of ocean wave model*

Significant wave height (SWH) is the most significant variable used to evaluate ocean wave model performance. Waves are relatively strong in the Southern Ocean, and northern Atlantic and northern Pacific oceans, while ocean waves are relatively weak in oceans in the low latitudes. There is also a marked seasonal cycle with SWH being larger in winter and smaller in summer. To evaluate ocean wave model performance, we compared model output with ERA5 reanalysis (Hersbach et al., 2019) from 1979–2009. Figure 11 shows that the FIO-ESM v2.0 OMIP-1 simulation can capture the basic spatial pattern and seasonal cycle of SWH in the ERA5 reanalysis dataset. The main model bias is found in regions with strong waves where simulated SWH is slightly lower than SWH from reanalysis. Mean error of simulated SWH is –0.01 m in January and –0.25 m in July. Root mean square error is 0.31 m and 0.41 m, respectively. In general, the MASNUM wave model works quite well in FIO-ESM v2.0.

Ocean surface waves are also undergoing considerable changes as global temperature increases. According to Young et al. (2011), satellite altimeter measurements indicate a consistent, weak and positive trend in SWH in the South Hemisphere between 1985 and 2008, and a weak and negative trend in large parts of the north Pacific and north Atlantic (see Fig. 1 in Young et al. (2011)). We reproduced Fig. 1 in Young et al. (2011) using output from the FIO-ESM v2.0 OMIP-1 simulation to evaluate model performance in long-term trend simulation (Fig. 12). Ocean wave simulations in FIO-ESM v2.0 OMIP-1 can adequately reproduce the long-term SWH trends reported by Young et al. (2011), giving us confidence to use FIO-ESM v2.0 fully-

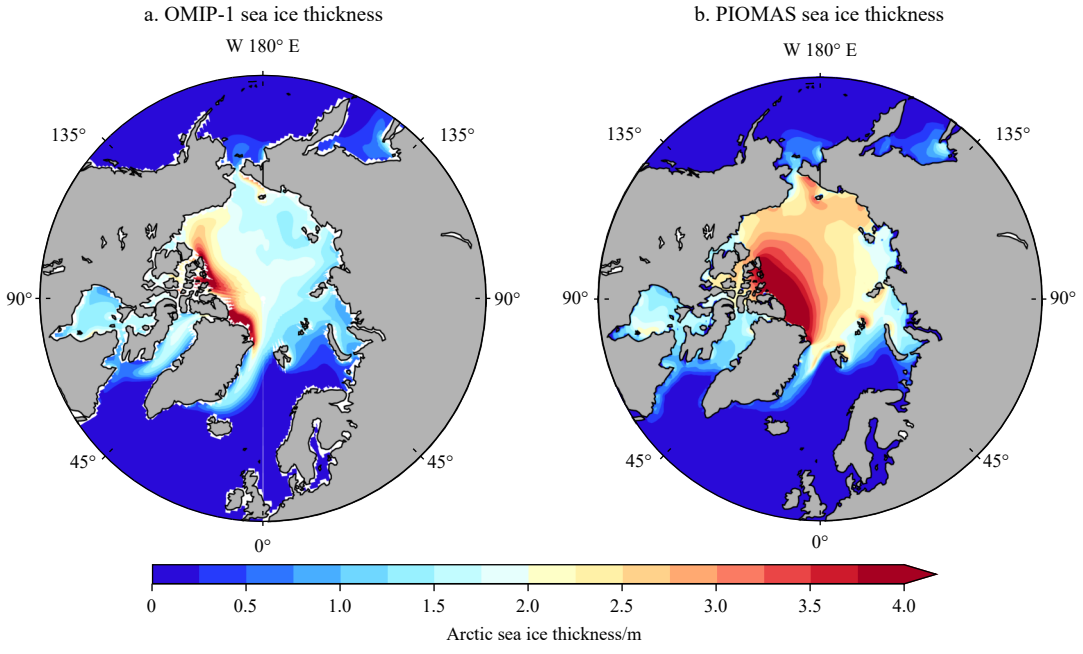

Fig. 10. Simulated Arctic sea ice thickness in March from the last cycle of the FIO-ESM v2.0 OMIP-1 simulation (a) and Pan-Arctic Ice-Ocean Modeling and Assimilation System (PIOMAS) (b).

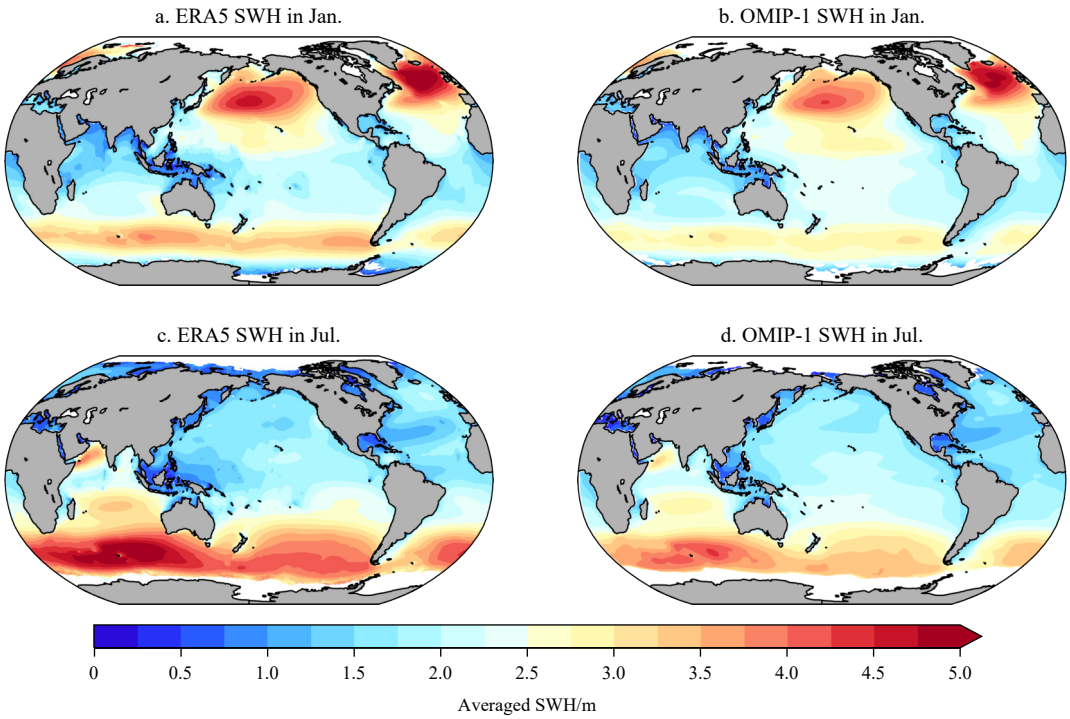

Fig. 11. Average significant wave height (SWH) from 1979–2009 obtained from ERA5 reanalysis (a, c), and the FIO-ESM v2.0 OMIP-1 simulation (b, d) in January (a, b) and July (c, d).

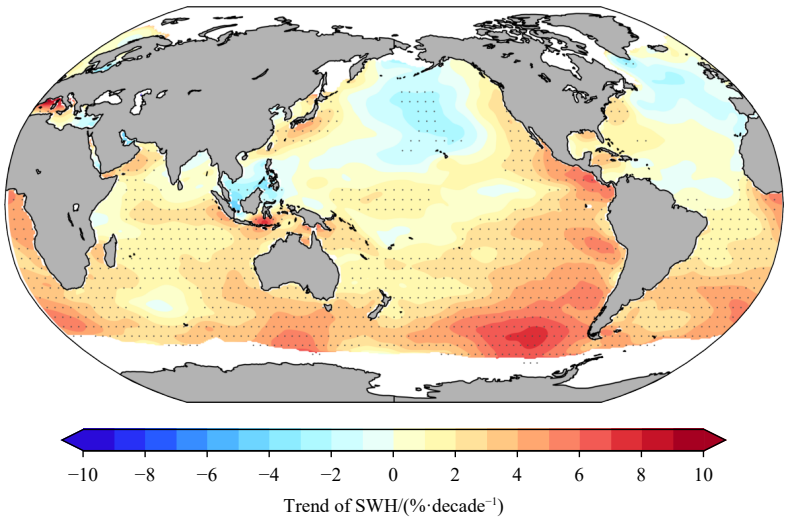

Fig. 12. Linear trends of OMTP-1 significant wave height (SWH) during 1985 to 2008. Dots indicate locations where linear trend exceeds 90% confidence level.

coupled simulations to project future changes in ocean surface waves as part of the CMIP6 Scenario Model Intercomparison Project.

4 Summary and discussion

In this study, we introduced the FIO-ESM v2.0 OMIP-1 experiment, and evaluated results of the simulation. Unlike other OMIP models, FIO-ESM v2.0 includes a coupled ocean surface wave component model that takes into account non-breaking wave-induced vertical mixing and effect of surface wave Stokes drift on air-sea momentum and heat fluxes. A sub-grid SST diurnal cycle parameterization was also employed to take into account the effect of SST diurnal cycle on air-sea heat and gas fluxes for improving simulations of air-sea interactions in the model.

Mean values and long-term trends of SWH were adequately reproduced in the FIO-ESM v2.0 OMIP-1 simulation. There is a reasonable fit between the SST diurnal cycle obtained from *in situ* observations and that parameterized by FIO-ESM v2. Model drift, bias in temperature, salinity and ocean mixed layer depth, and simulation of AMOC all suggest good model performance in the FIO-ESM v2.0 OMIP-1 experiment. However, the underestimated summer sea ice in both hemispheres in FIO-ESM v2.0 should be further improved in the future.

The ocean and sea ice outputs of the FIO-ESM v2.0 OMIP-1 experiment (Song et al., 2020) have been released and are available on the Earth System Grid Federation (ESGF) CMIP6 website (https://esgf-node.llnl.gov/search/cmip6/). Since ocean wave variables are not part of the standard CMIP6 variables, ocean wave output of the FIO-ESM v2.0 OMIP-1 experiment has not been released through the ESGF CMIP6 website. Three-hourly snapshot and monthly mean ocean surface wave variables (including significant wave height, wave direction, spectrum peak, and zero-crossing wave period) are available by contacting the corresponding author.

Acknowledgements

FIO-ESM v2.0 OMIP experiment was carried out at the Beijing Super Cloud Computing Center (BSCC). The WOA13 temperature and salinity, the observed mixed layer depth, RAPID AMOC observations, TOGA/COARE mooring observations, satellite observed sea ice extent, PIOMAS sea ice thickness data and reanalysis significant wave height dataset of ERA5 used in this study are from https://www.nodc.noaa.gov/OC5/woa13/, http://www.ifremer.fr/cerweb/deboyer/mld/Surface_Mixed_Layer_Depth.php, https://www.rapid.ac.uk/, www.pmel.noaa.gov, http://nsidc.org/data/g02135.html, http://psc.apl.uw.edu/research/projects/arctic-sea-ice-volume-anomaly/data/model_grid, and https://cds.climate.copernicus.eu/#!/home, respectively. We thank the above computing resource and data providers.

References

Bailey D, Holland M, Hunke E, et al. 2011. Community Ice CodE (CICE) user's guide version 4.0 released with CCSM 4.0. Tech rep, Los Alamos National Library

Bao Ying, Song Zhenya, Qiao Fangli. 2020. FIO-ESM Version 2.0: Model description and evaluation. Journal of Geophysical Research: Oceans, 125(6): e2019JC016036, doi: 10.1029/2019JC016036

Bernie D J, Guilyardi E, Madec G, et al. 2008. Impact of resolving the diurnal cycle in an ocean-atmosphere GCM: Part 2. A diurnally coupled CGCM. Climate Dynamics, 31(7–8): 909–925, doi: 10.1007/s00382-008-0429-z

Chen Siyu, Qiao Fangli, Huang Chuanjiang, et al. 2018. Effects of the non-breaking surface wave-induced vertical mixing on winter mixed layer depth in subtropical regions. Journal of Geophysical Research: Oceans, 123(4): 2934–2944, doi: 10.1002/2017JC013038

Clayson C A, Weitlich D. 2007. Variability of tropical diurnal sea surface temperature. Journal of Climate, 20(2): 334–352, doi: 10.1175/JCLI3999.1

Craig A P, Vertenstein M, Jacob R. 2012. A new flexible coupler for earth system modeling developed for CCSM4 and CESM1. The International Journal of High Performance Computing Applications, 26(1): 31–42, doi: 10.1177/1094342011428141

Dai Aiguo, Qian Taotao, Trenberth K E, et al. 2009. Changes in continental freshwater discharge from 1948 to 2004. Journal of Climate, 22(10): 2773–2792, doi: 10.1175/2008JCLI2592.1

Dai Aiguo, Trenberth K E. 2002. Estimates of freshwater discharge from continents: Latitudinal and seasonal variations. Journal of Hydrometeorology, 3(6): 660–687, doi: 10.1175/1525-7541(2002)003<0660:EOFDFC>2.0.CO;2

Danabasoglu G, Large W G, Tribbia J J, et al. 2006. Diurnal coupling in the tropical oceans of CCSM3. Journal of Climate, 19(11): 2347–2365, doi: 10.1175/JCLI3739.1

Danabasoglu G, Yeager S G, Bailey D, et al. 2014. North Atlantic simulations in coordinated ocean-ice reference experiments phase II (CORE-II): Part I. Mean states. Ocean Modelling, 73: 76–107, doi: 10.1016/j.ocemod.2013.10.005

Danabasoglu G, Yeager S G, Kim W M, et al. 2016. North Atlantic simulations in Coordinated Ocean-ice Reference Experiments phase II (CORE-II): Part II. Inter-annual to decadal variability. Ocean Modelling, 97: 65–90, doi: 10.1016/j.ocemod.2015.11.007

de Boyer Montégut C, Madec G, Fischer A S, et al. 2004. Mixed layer depth over the global ocean: An examination of profile data and a profile-based climatology. Journal of Geophysical Research: Oceans, 109(C12): C12003, doi: 10.1029/2004JC002378

Downes S M, Farneti R, Uotila P, et al. 2015. An assessment of Southern Ocean water masses and sea ice during 1988–2007 in a suite of interannual CORE-II simulations. Ocean Modelling, 94: 67–94, doi: 10.1016/j.ocemod.2015.07.022

Eyring V, Bony S, Meehl G A, et al. 2016. Overview of the Coupled Model Intercomparison Project Phase 6 (CMIP6) experimental design and organization. Geoscientific Model Development, 9(5): 1937–1958, doi: 10.5194/gmd-9-1937-2016

Fetterer F, Knowles K, Meier W, et al. 2017. Sea ice index, version 3. Boulder, CO, USA: National Snow and Ice Data Center, doi: 10.7265/N5K072F8

Frajka-Williams E, Moat B I, Smeed D A, et al. 2021. Atlantic meridional overturning circulation observed by the RAPID-MOCHA-WBTS (RAPID-Meridional Overturning Circulation and Heatflux Array-Western Boundary Time Series) array at 26N from 2004 to 2020 (v2020.1). British Oceanographic Data Centre-Natural Environment Research Council, doi: 10.5285/cc1e34b3-3385-662b-e053-6c86abc03444

Griffies S M, Biastoch A, Böning C, et al. 2009. Coordinated ocean-ice reference experiments (COREs). Ocean Modelling, 26(1–2): 1–46, doi: 10.1016/j.ocemod.2008.08.007

Griffies S M, Danabasoglu G, Durack P J, et al. 2016. OMIP contribution to CMIP6: Experimental and diagnostic protocol for the physical component of the Ocean Model Intercomparison Project. Geoscientific Model Development, 9(9): 3231–3296, doi: 10.5194/gmd-9-3231-2016

Ham Y G, Kug J S, Kang I S, et al. 2010. Impact of diurnal atmosphere-ocean coupling on tropical climate simulations using a coupled GCM. Climate Dynamics, 34(6): 905–917, doi: 10.1007/s00382-009-0586-8

Hersbach H, Bell B, Berrisford P, et al. 2019. Global reanalysis: Goodbye ERA-Interim, hello ERA5. ECMWF Newsletter 159, 17–24, https://www.ecmwf.int/en/newsletter/159/meteorology/global-reanalysis-goodbye-era-interim-hello-era5 [2019-04-01/2021-07-16]

Huang Chuanjiang, Qiao Fangli, Dai Dejun. 2014. Evaluating CMIP5 simulations of mixed layer depth during summer. Journal of Geophysical Research: Oceans, 119(4): 2568–2582, doi: 10.1002/2013JC009535

Huang Chuanjiang, Qiao Fangli, Shu Qi, et al. 2012. Evaluating austral summer mixed-layer response to surface wave-induced mixing in the southern Ocean. Journal of Geophysical Research: Oceans, 117(C11): C00J18, doi: 10.1029/2012JC007892

Huang N E. 1971. Derivation of Stokes drift for a deep-water random gravity wave field. Deep-Sea Research and Oceanographic Abstracts, 18(2): 255–259, doi: 10.1016/0011-7471(71)90115-X

Ilıcak M, Drange H, Wang Qiang, et al. 2016. An assessment of the Arctic Ocean in a suite of interannual CORE-II simulations. Part III: Hydrography and fluxes. Ocean Modelling, 100: 141–161, doi: 10.1016/j.ocemod.2016.02.004

Kawai Y, Wada A. 2007. Diurnal sea surface temperature variation and its impact on the atmosphere and ocean: A review. Journal of Oceanography, 63(5): 721–744, doi: 10.1007/s10872-007-0063-0

Kobayashi S, Ota Y, Harada Y, et al. 2015. The JRA-55 reanalysis: General specifications and basic characteristics. Journal of the Meteorological Society of Japan, 93(1): 5–48

Large W G, McWilliams J C, Doney S C. 1994. Oceanic vertical mixing: a review and a model with a nonlocal boundary layer parameterization. Reviews of Geophysics, 32(4): 363–403, doi: 10.1029/94RG01872

Large W G, Yeager S G. 2009. The global climatology of an interannually varying air–sea flux data set. Climate Dynamics, 33(2–3): 341–364, doi: 10.1007/s00382-008-0441-3

Locarnini R A, Mishonov A V, Antonov J I, et al. 2013. World ocean at-

las 2013. Volume 1: Temperature. Silver Spring: National Oceanic and Atmospheric Administration

Lumpkin R, Speer K. 2007. Global ocean meridional overturning. Journal of Physical Oceanography, 37(10): 2550–2562, doi: 10.1175/JPO3130.1

Masson S, Terray P, Madec G, et al. 2012. Impact of intra-daily SST variability on ENSO characteristics in a coupled model. Climate Dynamics, 39(3–4): 681–707, doi: 10.1007/s00382-011-1247-2

Qiao Fangli, Song Zhenya, Bao Ying, et al. 2013. Development and evaluation of an Earth System Model with surface gravity waves. Journal of Geophysical Research: Oceans, 118(9): 4514–4524, doi: 10.1002/jgrc.20327

Qiao Fangli, Yuan Yeli, Ezer T, et al. 2010. A three-dimensional surface wave-ocean circulation coupled model and its initial testing. Ocean Dynamics, 60(5): 1339–1355, doi: 10.1007/s10236-010-0326-y

Qiao Fangli, Yuan Yeli, Yang Yongzeng, et al. 2004. Wave-induced mixing in the upper ocean: Distribution and application to a global ocean circulation model. Geophysical Research Letters, 31(11): L11303

Qiao Fangli, Zhao Wei, Yin Xunqiang, et al. 2016. A highly effective global surface wave numerical simulation with ultra-high resolution. In: SC'16: Proceedings of the International Conference for High Performance Computing, Networking, Storage and Analysis. Salt Lake City, UT, USA: IEEE, 46–56

Rascle N, Ardhuin F, Queffeulou P, et al. 2008. A global wave parameter database for geophysical applications: Part 1. Wave-current–turbulence interaction parameters for the open ocean based on traditional parameterizations. Ocean Modelling, 25(3–4): 154–171, doi: 10.1016/j.ocemod.2008.07.006

Shu Qi, Qiao Fangli, Song Zhenya, et al. 2011. Improvement of MOM4 by including surface wave-induced vertical mixing. Ocean Modelling, 40(1): 42–51, doi: 10.1016/j.ocemod.2011.07.005

Shu Qi, Wang Qiang, Su Jie, et al. 2019. Assessment of the Atlantic water layer in the Arctic Ocean in CMIP5 climate models. Climate Dynamics, 53(9–10): 5279–5291, doi: 10.1007/s00382-019-04870-6

Smith R, Jones P, Briegleb B P, et al. 2010. The Parallel Ocean Program (POP) reference manual: ocean component of the Community Climate System Model (CCSM), https://www.cesm.ucar.edu/models/cesm2/ocean/doc/sci/POPRefManual.pdf [2010-03-23/2021-06-01]

Song Z, Qiao F, Bao Y, et al. 2020. FIO-QLNM FIO-ESM2.0 model output prepared for CMIP6 OMIP OMIP 1. Version 20200324. Earth System Grid Federation, doi: 10.22033/ESGF/CMIP6.9201

Tsujino H, Urakawa L S, Griffies S M, et al. 2020. Evaluation of global ocean-sea-ice model simulations based on the experimental protocols of the Ocean Model Intercomparison Project phase 2 (OMIP-2). Geoscientific Model Development, 13(8): 3643–3708, doi: 10.5194/gmd-13-3643-2020

Tsujino H, Urakawa S, Nakano H, et al. 2018. JRA-55 based surface dataset for driving ocean-sea-ice models (JRA55-do). Ocean Modelling, 130: 79–139, doi: 10.1016/j.ocemod.2018.07.002

Wang Shizhu, Wang Qiang, Shu Qi, et al. 2019. Improving the upper-ocean temperature in an ocean climate model (FESOM 1.4): Shortwave penetration versus mixing induced by nonbreaking surface waves. Journal of Advances in Modeling Earth Systems, 11(2): 545–557, doi: 10.1029/2018MS001494

Wang Yonggang, Qiao Fangli, Fang Guohong, et al. 2010. Application of wave - induced vertical mixing to the K profile parameterization scheme. Journal of Geophysical Research: Oceans, 115(C9): C09014

Webster P J, Lukas R. 1992. TOGA COARE: the coupled ocean-atmosphere response experiment. Bulletin of the American Meteorological Society, 73(9): 1377–1416, doi: 10.1175/1520-0477(1992)073<1377:TCTCOR>2.0.CO;2

Yang Xiaodan, Song Zhenya, Tseng Y H, et al. 2017. Evaluation of three temperature profiles of a sublayer scheme to simulate SST diurnal cycle in a global ocean general circulation model. Journal of Advances in Modeling Earth Systems, 9(4): 1994–2006, doi: 10.1002/2017MS000927

Young I R, Zieger S, Babanin A V. 2011. Global trends in wind speed and wave height. Science, 332(6028): 451–455, doi: 10.1126/science.1197219

Zhang Jinlun, Rothrock D A. 2003. Modeling global sea ice with a thickness and enthalpy distribution model in generalized curvilinear coordinates. Monthly Weather Review, 131(5): 845–861, doi: 10.1175/1520-0493(2003)131<0845:MGSIWA>2.0.CO;2

Zweng M M, Reagan J R, Antonov J I, et al. 2013. World ocean atlas 2013. Volume 2: Salinity. Silver Spring, ML, USA: National Oceanic and Atmospheric Administration